

AperTO - Archivio Istituzionale Open Access dell'Università di Torino

Morphological examination and transcriptomic profiling to identify prednisolone treatment in beef cattle

This is the author's manuscript

Original Citation:

Availability:

This version is available <http://hdl.handle.net/2318/1611715> since 2017-11-24T10:23:16Z

Published version:

DOI:10.1021/acs.jafc.6b02996

Terms of use:

Open Access

Anyone can freely access the full text of works made available as "Open Access". Works made available under a Creative Commons license can be used according to the terms and conditions of said license. Use of all other works requires consent of the right holder (author or publisher) if not exempted from copyright protection by the applicable law.

(Article begins on next page)

This is the author's final version of the contribution published as:

Cannizzo, Francesca T; Pegolo, Sara; Pregel, Paola; Manuali, Elisabetta; Salamida, Sonia; Divari, Sara; Scaglione, Frine E; Bollo, Enrico; Biolatti, Bartolomeo; Bargelloni, Luca. Morphological examination and transcriptomic profiling to identify prednisolone treatment in beef cattle. JOURNAL OF AGRICULTURAL AND FOOD CHEMISTRY. 64 (44) pp: 8435-8446.
DOI: 10.1021/acs.jafc.6b02996

The publisher's version is available at:

<http://pubs.acs.org/doi/pdf/10.1021/acs.jafc.6b02996>

When citing, please refer to the published version.

Link to this full text:

<http://hdl.handle.net/>

Research Article

Morphological examination and transcriptomic profiling to identify prednisolone treatment in beef cattle.

Francesca T. Cannizzo ^a, Sara Pegolo ^b, Paola Pregel ^{a,*}, Elisabetta Manuali ^c, Sonia Salamida ^c, Sara Divari ^a, Frine E. Scaglione ^a, Enrico Bollo ^a, Bartolomeo Biolatti ^a, Luca Bargelloni ^b

^a*Dipartimento di Scienze Veterinarie, Università degli Studi di Torino, Largo P. Braccini 2, 10095 Grugliasco (TO), Italy*

^b*Dipartimento di Biomedicina Comparata e Alimentazione, Università di Padova, Viale dell'Università 16, 35020 Legnaro, Padova, Italy*

^c*Istituto Zooprofilattico Sperimentale dell'Umbria e delle Marche, Via G. Salvemini 1, 06126 Perugia, Italy*

*Corresponding author. Tel.: +39 0116709044.

E-mail address: paola.pregel@unito.it (P. Pregel).

Abstract

In livestock production corticosteroids are licensed only for therapy, nevertheless they are often illegally used as growth promoters. The aim of this study was to identify morphological or biomolecular alterations induced by prednisolone (PDN) in experimentally treated beef cattle, since PDN and its metabolites are no longer detectable by LC-MS/MS methods in biological fluids. Moreover, PDN do not induce any histological alterations in thymus, differently from Dexamethasone treatments. Therefore, a marker of illicit treatment for this growth promoter could be useful. Eight male Italian Friesian beef cattle were administered prednisolone acetate 30 mg day⁻¹ *per os* for 35 days, while seven beef cattle represented the control group. Six days after drug withdrawal the animals were slaughtered. Morphological and morphometric modifications were evaluated in epididymis and testis, whereas transcriptomic changes induced by PDN administration were investigated in Peripheral Blood Mononuclear Cells (PBMCs) at different sampling times, and in skeletal muscle and testis sampled at slaughtering. In the epididymis, spermatozoa number decreased in PDN treated animals, and in some cases they were totally absent. Correspondently, in testis of treated animals, down-regulation for serine/threonine kinase 11 (STK11) gene expression was detected ($p < 0.01$). DNA microarray analysis revealed a total of 133 differentially expressed genes in skeletal muscle and testis, and 907 and 1,416 in PBMCs after 33 days of treatment and at slaughtering, respectively. Histological investigations on epididymal content could represent a promising marker for PDN treatment in beef cattle, and could be used as a screening method in order to identify animals worthy of further investigation with official methods. Moreover, the clear transcriptomic signature of PDN treatment evidenced in PBMCs supported for the possibility of using this matrix to monitor the illicit treatment *in vivo* during ranching.

Keywords: cattle, growth promoters, microarray, morphometry, prednisolone

Introduction

Dexamethasone (DEX) and prednisolone (PDN) are corticosteroids (CSs) frequently used in livestock production. They are licensed for therapy in human and veterinary medicine due to their anti-inflammatory and immunosuppressive properties¹. Moreover, CSs are often illegally used as growth promoters in animal husbandry, usually at low dosages and by oral administration, either alone or in cocktails containing different anabolic agents². To protect consumer's health, European Union established maximum residue limits for these CSs in several biological matrices, such as muscle, kidney, liver and milk from different species³. Since 2008, the Italian National Program for Residue Surveillance (PNR) has detected a marked increase of cattle positive for CS treatments, including PDN⁴. Due to the rapid metabolism and excretion of PDN, the analyses of its residues by LC/MS-MS are not suitable. The Italian Ministry of Health introduced thymus histological examination as a screening test⁵, in order to identify DEX illegal treatments in cattle, since DEX induces thymus atrophy⁶⁻¹⁰. Unfortunately, PDN illegal treatments does not induce thymus morphological alterations in beef cattle¹¹; moreover, gene expression profiling by DNA-microarray on thymus has revealed to be a weak tool to detect the illegal use of PDN¹². Consequently, new reliable tests would be helpful to reveal PDN abuse in livestock production.

The aim of this study was to recognize alterations induced by PDN treatment in other biological matrices. Morphological and morphometric modifications were evaluated in epididymis and testis, whereas transcriptomic signatures of PDN administration were investigated in Peripheral Blood Mononuclear Cells (PBMCs), skeletal muscle (*Biceps brachii*) and testis collected from experimentally treated beef cattle, in order to identify and recognize potential biomarkers to be used for screening purposes.

Material and methods

Animals and Experimental Design

Experimental design was already described in details by Cannizzo *et al.*¹². Briefly, fifteen male Italian Friesian beef cattle (9-17 month-old) were randomly assigned to two groups: group P (n = 8) was administered prednisolone acetate (PA, Novosterol, Italy) 30 mg day⁻¹ *per os* for 35 days, from day 51 to day 85, while group K (n = 7) represented the control group. Six days after drug withdrawal the animals were slaughtered. The experiment was authorized by the Italian Ministry of Health and the Ethics Committee of the University of Turin and the carcasses of the treated beef cattle were appropriately destroyed¹³.

Animals were weighed before first treatment and the day before slaughtering and weight gain was recorded, as reported in Cannizzo *et al.*¹². Relative testis weight was calculated as testis weight (g)/animal weight (kg) ratio.

PBMCs isolation

Blood samples were collected from each animal with evacuating tubes containing acid-citrate-dextrose (ACD) as anticoagulant from the external jugular vein at 0 (T0), 51 (T1), 61 (T2), 84 (T3), and 92 (T4) days (Fig. 1). The PBMCs were isolated on Ficoll-gradient as previously described¹⁴. PBMCs were pelleted by centrifugation, and resuspended in RNeasy® (Thermo Fisher Scientific, MA, USA). Pellet was frozen in TRIzol Reagent (Thermo Fisher Scientific) at -80°C until RNA extraction.

Post mortem tissue sampling and processing

At slaughtering, samples from *Biceps brachii* muscle, testis and caudal epididymis were collected from each animal and opportunely stored for subsequent investigations. For histological analysis testicular and epididymal tissues were immediately fixed in Bouin-Hollande solution for approximately 24 h, then dehydrated in ethanol, paraffin embedded, and sectioned at 4 µm. Haematoxylin and eosin (HE) stained sections were observed under a light microscope, and submitted to morphometric analysis and immunohistochemistry for Ki67. Samples from testis and

epididymis were also glutaraldehyde fixed and ultrastructural features were examined by transmission electron microscopy (TEM). For TEM analysis the samples were cut into small pieces (2x2 mm), fixed in 2.5% glutaraldehyde (TAAB, England) at 4°C in PBS pH 7.4 for 2 h, and post fixed in 1% tetroxide osmium (OsO₃) (Next Chimica, South Africa) at 4°C in PBS for 2 h. The tissues were then dehydrated through ascending grades of ethanol, incubated in propylene oxide (TAAB) at room temperature for 5 min and embedded in Epon 812 (TAAB). Resin blocks were solidified at 60°C for 48 h. Semithin sections (1 µm) were cut and stained with 1% toluidine blue (w/v) pH 3.5. Silver coloured ultrathin sections (60-70 nm) were collected onto copper grids coated with a Formvar layer (EMS, PA, USA) and double stained with uranyl acetate and lead citrate. Microphotographs were obtained at 80 kV on a CM12 STEM electron microscope (Philips).

For gene expression analysis a portion of skeletal muscle and testis (approximately 100 mg) was immediately fixed in RNAlater[®] and stored at -80°C.

Morphometric Analysis

Morphometric analyses on testis and epididymis samples were performed on HE stained sections. Digital microphotographs were obtained with a Nikon DS-Fi1 color digital camera (Nikon Instruments, Italy), at 200x magnification for testis and at 600x for epididymis under a light microscope. For testis, at least 40 randomly selected complete tubules per animal were examined using Image-Pro Plus software (Media Cybernetics, MD, USA). Seminiferous tubular equivalent diameter (STED), seminiferous epithelial height (SHE), area occupied by the seminiferous tubules and interstitial area were evaluated. Furthermore, the number of Sertoli cells, spermatogonia, spermatocytes, immature and mature spermatids and immature spermatozoa (ready to be released) present in at least 30 tubules for each animal were annotated, analyzing sections at 400x magnification. For epididymis, at least 25 randomly selected ducts per animal were examined and the epithelial height was recorded.

Evaluation and quantification of cell proliferation

Immunohistochemical staining for Ki67 antigen was performed to evaluate proliferating cells on testis sections. Endogenous peroxidases were inactivated and antigen retrieval was performed with citrate buffer 10 mM, pH 6.0 at 98°C for 40 min in a water bath. The sections were subsequently incubated at room temperature with anti-Ki67 monoclonal antibody (1:50 in PBS) (clone MIB-1, Dako, Italy) for 90 min. The staining was visualized with the Dako REAL EnVision Detection System (K5007, Dako, Italy) by a Dako Autostainer (Dako). Ten randomly selected fields for each section were analyzed, after taking microphotographs at 200x magnification by light microscopy, using Image-Pro Plus software. The area of Ki67-positive nuclei was recorded and expressed as a percentage (mean \pm sd).

Detection of apoptosis in testis

From each animal 4 μ m thick sections of testis were stained using the ApopTag In Situ Apoptosis Detection Kit (Merck Millipore, MA, USA) according to the manufacturer's instructions. The immunohistochemical TUNEL (terminal uridine deoxynucleotidyl transferase dUTP nick-end labeling) staining was used to reveal the apoptotic nuclei, counterstaining the reaction with methyl green 0.5 per cent (w:v) for 10 minutes, and destaining in n-butanol.

RNA extraction

Samples of testis, skeletal muscle and PBMCs were treated with TRIzol Reagent (Ambion®, Thermo Fisher Scientific) and, in order to remove DNA contamination, the extracted RNA was subjected to DNase digestion with the QIAGEN RNase-Free DNase Set (Qiagen, Germany). RNA purification was performed with the RNeasy MinElute Cleanup Kit (Qiagen, Germany). The concentration of RNA samples was determined by a UV-Vis spectrophotometer NanoDrop ND-1000 (Nanodrop Technologies, DE, USA) and RNA integrity was checked using an

Agilent 2100 Bioanalyzer (Agilent Technologies, CA, USA). Only RNA samples with RNA integrity number (RIN) ≥ 7.0 were included in the analysis.

Relative quantification of STK11 by qPCR

cDNA was synthesized from 1 μ g of total RNA using the QuantiTect Reverse Transcription Kit (Qiagen, Germany). The relative amounts of specific *Bos taurus* serine/threonine kinase 11 (STK11) mRNA (XM_003586293) was calculated submitting the cDNA to qPCR¹⁵ with an IQ5 detection system (BioRad) using IQ SYBR Green Supermix (BioRad, CA, USA). Primer sequences of STK11 were designed using Primer 3 (vers. 0.4.0)¹⁶ (forward: GACAGTGATGCCCTACCTGG, reverse: GGCACTGTGAAGTCCTGAGT, amplicon size 108 bp). The peptidylprolyl isomerase A (PPIA) gene was used as a housekeeping gene control as previously reported¹⁷.

After confirming that target and housekeeping gene amplifications had similar efficiencies, gene expression levels were determined using a relative quantification assay, using the comparative Cq method ($\Delta\Delta Cq$ method)¹⁸. Then, the relative abundances of each transcript were calculated as $2^{-\Delta\Delta Cq}$ (fold increase)¹⁹⁻²¹, normalised to PPIA and relative to the control sample.

RNA amplification, labeling and hybridization

Sample labeling and hybridization were performed according to the Agilent One-Color Microarray-Based Gene Expression Analysis protocol, as reported in details in Pegolo *et al.* (2012). Briefly, 200 ng of total RNA were linearly amplified for each sample and labeled with Cy3-dCTP. Microarray data have been deposited in NCBI's Gene Expression Omnibus²² (GSE50037, GEO Series accession number).

Normalization of microarray data

Microarray data extraction was performed using the standard procedures of the Agilent Feature Extraction Software version 9.5.1. On the basis of the uniformity of the Spike-in intensities

across the samples, all samples (negative and treated samples) were normalized together in a single run using the cyclic LOWESS (Locally-weighted Regression) normalization procedure.

After normalization, an additional quality control step was introduced to remove probes with intensity values lower than the second lowest spike-in concentration in the 70% of samples, as this value was considered too close to the limit of detection. The cut-off intensity values corresponded to 3.5 for muscle and testis samples and to 4 for PBMCs samples. This filtering step resulted in the removal of 1,350, 4,162 and 4,318 unique transcripts for testis, muscle and PBMCs, respectively.

Filtering and normalization procedures were performed using R statistical software, available at <http://www.r-project.org/>.

Statistical analyses

t-test or the non parametric Mann-Whitney Test were performed using GraphPad InStat (vers. 3.05) statistical software (GraphPad, CA, USA). The Grubbs test was used to exclude potential outliers. A p value of <0.05 was considered to be statistically significant.

Differential expression of microarray data was tested by t-test statistics using TMEV suite²³ and the differentially regulated genes (DEG) were identified on the basis of a false discovery rate (FDR) <0.05 and a fold change (FC) >1.5 . Sample class prediction was implemented using the program PAM²⁴, available online at <http://www.stat.stanford.edu/~tibs/PAM>.

Functional enrichment analysis

The Functional Annotation tool available in the DAVID Database (<http://david.abcc.ncifcrf.gov/>) was adopted to carry out the enrichment analysis on the differentially up- and down-regulated genes. All GO terms and KEGG (Kyoto Encyclopedia of Genes and Genomes) pathways included in the DAVID knowledgebase were included. For KEGG terms, GO Biological Process (BP_FAT) and Molecular Function (MF_FAT), the following parameters were selected: gene count 4, ease 0.05.

Results

Animal welfare and livestock performances

As already reported by Cannizzo *et al.*¹², when compared to the control group, weight gains were larger in group treated with PDN ($p = 0.0047$), indicating that the animals responded to PDN administration. Also, the average daily gain was higher in group P, compared to group K (1.587 vs. 1.178 kg/day; $P = 0.007$), whereas relative testis weight did not vary between treated animals and controls (0.583 ± 0.117 vs. 0.606 ± 0.051 g/kg).

Testis morphological features

Morphological and ultrastructural analyses of testis showed a wide heterogeneity of tubular epithelium appearance in animals belonging to group P. The interstitium did not show significant alterations. Lesions were totally absent in three cases, whereas they heavily characterized the other treated animals. Two cases showed an apparently reduced SHE, whereas in other animals the germ line appeared complete. Both light microscopy and TEM revealed in group P a prominent vacuolization of the seminiferous epithelium near the basement membrane towards Sertoli cells (Figs. 2b and 3b).

Ultrastructurally, the vacuolated spaces observed in the region between the basement membrane and the basal epithelial layer revealed cytoplasmic contractions that shrink the intercellular spaces between Sertoli cell and the neighboring germ cells with formation of membrane-bounded vacuoles encircled by processes of Sertoli cells. The germinal epithelium rested on a basement membrane with an irregular arrangement (Fig. 3b). Moreover, the degeneration of the superficial layer characterized by cells fragmentation and anucleation was also evident. Spermatids appeared swollen, filled with vacuoles containing cellular debris that pushed the eccentrically placed nuclei, indicating a vacuolar degeneration of these germ cells. Retained and altered spermatids with nuclear vacuoles were identified in the basal compartment of the epithelium

and embedded in Sertoli cells, that exhibited severe destruction and rarefaction of cytoplasm. No Sertoli cell and spermatid plasma membranes were visible, suggesting a possible phagocytic activity (Figs. 3 c-d).

Epididymis morphological features

In control group the epithelium of epididymis consisted of tall columnar principal cells (PC), that exhibited a highly developed secretory and endocytic apparatus, and basally aligned nuclei. Stereocilia were abundant and the epididymal ducts appeared filled with spermatozoa (Figs. 2 c-e). PC showed apical cytoplasmic protrusions referred to apical blebs that originated by apocrin secretion. Ultrastructurally, the apical blebs were found along the entire epididymis and they were characterized by heterogeneous shape and size at the apical surface of PC. These protrusions were directed towards the luminal compartment and contained several types of organelles, embedded in a homogeneous matrix. The blebs detached from the PC and entering the lumen, showed fragmentation and formation of aposomes, spherical membrane-bound bodies, closely related to spermatozoa. Aposomes contained electron dense particles and heterogeneous membrane-bounded vesicles, termed epididymosomes, that gave them different grades of electron density (Figs. 3 e-f)²⁵⁻²⁶.

As in control tissues, in animals belonging to group P the ultrastructural features of the lining epithelium revealed well developed secretory cells, with no apparent morphological differences. However, the most striking feature observed in treated group was related to the intraluminal compartment, where the spermatozoa number decreased significantly, up to disappear, and this reduction was accompanied by an increased presence of cellular debris (Fig. 2). Under TEM observation, the apocrin protrusions consisted of membrane-bound balloons containing a proteinaceous material and blebbing at the apical pole of secretory cells (Figs. 3 g-h).

Morphometric Analysis

Morphometric analyses on light microscopy showed an increase ($p<0.05$) of the area occupied by the seminiferous tubules in group P compared to controls (80.9 ± 2.2 vs. 75.3 ± 4.7 % of examined area). On the contrary, STED and SHE did not vary significantly between the groups (respectively, P vs K, 253.9 ± 19.1 vs. 250.2 ± 16.5 μm and 72.0 ± 5.9 vs. 73.4 ± 8.3 μm). Neither the epithelial height of epididymal ducti varied significantly between the groups (P vs. K 80.1 ± 19.1 vs. $88.6\pm11.3\mu\text{m}$).

The mean number of Sertoli cells, spermatogonia, spermatocytes, mature and immature spermatids per tubule section did not vary between the groups; group P showed a greater number of immature spermatozoa compared to controls ($p<0.05$) (Fig. 4).

Evaluation and quantification of cell proliferation and apoptosis

Immunohistochemical staining for Ki67 antigen did not reveal any significant difference between groups P and K, even if the percentage of the positive nuclear area was higher in control group than in PDN treated animals (2.105 ± 0.89 % vs. 1.525 ± 0.88 %).

TUNEL assay did not reveal appreciable amounts of apoptotic cells, neither in group K nor in group P.

Relative gene expression of STK11 in testis

Administration of PDN induced a down-regulation ($p<0.01$) of the STK11 gene in testis by 1.87-fold in group P compared to control group. Normalized fold expression ($2^{-\Delta\Delta C_q}$) for P group was 0.534 ± 0.170 .

Microarray data analysis

After data extraction, normalization, and filtering, microarray data between group P and group K were compared for all the biological matrices under investigation. In skeletal muscle and

testis, t-test statistics evidenced a total of 133 genes differentially expressed. Considering PBMCs, 907 genes were differentially expressed at T3 and 1,416 T4 (Table 1).

The functional analyses were performed on the DEG lists obtained for all the comparisons. In testis, analysis of gene function using Functional Annotation tool in DAVID did not reveal specific pathways significantly enriched in testis samples from PDN-treated animals. Nevertheless, DEG were found to be variously involved in the olfactory transduction (6 genes), as well as regulators of calcium homeostasis (6 genes), xenobiotic metabolism (5 genes), immune system regulation (12 genes), and apoptosis and cell cycle regulation (8 genes) (Table 2). The functional analysis of the DEG in skeletal muscle samples revealed a weak regulation of single unrelated genes at the most (Table 3). On the other hand, enrichment analysis using the Functional Annotation tool in DAVID recognized several GO terms and KEGG pathways significantly enriched in PBMCs samples from both sampling times (Tables 4 and 5).

A statistical approach for class prediction implemented in PAM software was applied to microarray expression data of all PBMCs samples (both sampling times, treated animals and controls) to evaluate the ability of sample classification. Firstly, a discriminant analysis was performed on selected samples (both controls and treated animals; Training Sample Set) to identify the smallest panel of genes which provided the smallest misclassification error. Cross-validation allows to evaluate the accuracy of class prediction on the Training Sample Set (10% of samples were randomly extracted and classification was based on the discriminant function calculated on the residual cases). PAM enabled to exactly discriminate the two classes (controls and treated animals) for 93% of samples using only 36 genes out of 17,157 (Fig. 5; Table 6).

Discussion

For many years several research groups have attempted to identify molecular markers useful to detect different anabolic treatments in cattle²⁷⁻³¹. The usefulness of histological analyses on thymus morphology as a screening tool to identify illegal DEX treatments in cattle was already

established⁶⁻¹⁰. On the contrary, gross and histopathological investigations on thymus were not useful to detect anabolic treatments with PDN in beef cattle¹¹, and even gene expression profiling by DNA-microarray on thymus has revealed to be a weak tool¹². In the same study, no PDN residues were found in the urine of treated animals, probably because of PDN rapid metabolism and excretion, and of the suspension of the treatment. Due to the scarce results obtained with thymus, the authors investigated on other biological matrices the potential alterations induced by PDN anabolic treatment, in order to identify and recognize potential biomarkers to be used for screening purpose. Reproductive tract, i.e. epididymis and testis, was analyzed to detect morphological and morphometric modifications. Moreover, transcriptomic signatures of PDN administration were investigated in PBMCs, skeletal muscle and testis.

Testis relative weight did not vary between PDN treated animals and controls. Morphologic and ultrastructural appearance of testicular tissues was not exhaustive in identifying treatments, since the findings were very different from one animal to the other. Three cases were totally similar to animals of group K, whereas lesions heavily characterized the other treated animals, delineating a significant impact of treatment especially on spermatids. Morphometric analyses only revealed a significantly higher number of immature spermatozoa and an increase of the percentage of the area occupied by the seminiferous tubules in PDN treated beef calves compared to controls. Moreover, in the intraluminal compartment of epididymis, spermatozoa concentration decreased significantly up to disappear, whereas an increased presence of cellular debris was recorded.

The expression of STK11, also known as LKB1, in mammalian testis was demonstrated to be an essential regulator of spermatozoa release during spermiation³². This serine/threonine kinase is implicated in a number of key cellular processes. During the final phase of spermatogenesis, termed spermiation, mature spermatids detach from the supporting Sertoli cells and are released into the lumen of the seminiferous tubule. Denison *et al.*³² showed that spermiation is defective in the absence of LKB1. To the authors' best knowledge this protein has never been investigated in bovine testis. The gene expression analysis showed in PDN treated animals a significant down-regulation

for this gene. This data supports the hypothesis that the PDN treatment did not affect the production of mature spermatids, but it interfered with spermiation, probably involving STK11 pathway. The outcomes were represented by an apparently “healthy” morphology of testis, along with a huge decrease of spermatozoa in epididymis. These findings should be further investigated in order to verify if the association of morphometric analyses on testis and epididymis with STK11 expression could represent a useful marker for PDN treatment.

Immunohistochemical staining for Ki67 antigen on testicular and epididymal tissues did not reveal a significant difference between group P and K, even if the percentage of the positive nuclear area was higher in K group. TUNEL assay did not reveal appreciable amounts of apoptotic cells, nor in group K and in group P.

DNA microarray analysis identified a small set of differentially expressed genes between controls and PDN-treated animals in both testis and skeletal muscle samples.

In testis samples, apoptosis pathway and/or cell cycle regulation seemed to be affected by the treatment even if the weak differences observed could not explain the histological findings of testis samples. However, up-regulation of tumour necrosis factor receptor superfamily member 10A (TNFRSF10A) was observed. This receptor is activated by tumour necrosis factor-related apoptosis inducing ligand (TNFSF10/TRAIL), inducing cell apoptosis. Testicular germ cells, and specifically spermatocytes, were shown to be sensitive to TRAIL-mediated apoptosis. In reproductive tissues, a well-characterized apoptotic pathway involves the signal transduction pathway of Fas³³, a receptor which induces apoptosis after binding its ligand (FasL, up-regulated in PDN-treated animals) through an autocrine/paracrine signaling pathway³⁴.

Interestingly, olfactory transduction pathway was also regulated with 6 differentially expressed genes (Table 2). Surprisingly, a high number of olfactory receptors (ORs) expressed genes was found in the human testis and OR genes were shown to be more highly expressed in testis than in any other tissue³⁵. A putative role for some members of this family in regulation of sperm motility was evidenced. In particular, various bioassays evidenced that the activation of

hOR17-4 and mOR23 in human and mouse sperm, respectively, mediated flagellar motion patterns and chemotactic behavior³⁶.

Regulation of genes involved in the xenobiotic metabolism was observed as well. In particular, some cytochrome P450 (CYP) isoforms (CYP11B2, CYP4F2, and CYP24A1) and one phase II enzyme (sulfotransferase family, cytosolic, 1C, member 2, SULT1C2) were up-regulated after the PDN treatment. Glucocorticoids play an important role in the control of Leydig cell function, but they have been associated to an impairment of the steroidogenic pathway, when in excess (even following DEX administration)³⁷. Testis expresses many drug-metabolizing enzymes, whose various physiological functions are not definitely known. Some isoforms are involved in xenobiotic drug metabolism, thereby probably determining testicular toxicity³⁸. In cattle testis the administration of DEX alone or in combination with 17beta-oestradiol regulated the expression of some CYP isoforms (i.e. CYP1A1, CYP2E1, CYP17A1) and related transcription factors(e.g. peroxisome proliferator-activated receptor alpha)³⁹⁻⁴⁰, suggesting the potential usefulness of testis in the screening of drugs abuse in livestock farming.

Very poor information could be extrapolated from microarray results in skeletal muscle tissue, apart from the confirmation of a putative bias towards cell differentiation rather than proliferation which was already showed for other anabolic growth promoter treatments⁴¹⁻⁴². The PDN treatment seemed indeed to affect single unrelated genes in bovine muscle rather to regulate more complex pathways or processes.

The analysis of the microarray data relative to the bovine PBMCs collected at different sampling times revealed instead more interesting information. In particular, cytokine-cytokine receptor interaction pathway was significantly enriched at both sampling times with 18 and 20 genes differentially expressed at T3 and T4, respectively. The analysis of the regulated cytokines seemed to suggest that the PDN treatment produced a more polarized response of Th2 at T3, e.g. IL4-receptor (IL4R), IL10R-alpha, IL2RG, transforming growth- factor beta 1, IL1R antagonist were over-expressed, and gamma interferon was down-regulated. On the other hand, at T4 no

marked shift towards a specific T-helper sub-population seemed to occur, e.g. IL6R, IL15 and IL7 were over-expressed and gamma interferon receptor alpha 2 and IL2 were down-regulated. IL2 receptor signaling regulates tolerance and immunity. IL2 contributes to T-cell dependent activity, influencing CD8+ T cells activity, terminal differentiation of effector cells in primary response, and memory recall responses. IL2 is also the major cytokine contributing to the homeostasis of peripheral Treg cells: It is linked to Treg cells fitness maintaining both homeostasis and the suppressive program through induction of signal transducer and activator of transcription 5 (STAT5; STAT5B was up-regulated in PBMCs at T3), which directly contributes to forkhead box P3 transcription⁴³. In addition, it is known that glucocorticoid receptor associates with several transcription factor complexes which are regulated by signal transduction, such as STAT5⁴⁴. Up-regulation of IL2RG, STAT5B and many Th2 cytokines seemed to suggest a putative shift towards immune tolerance and anti-inflammatory pathways at T3. This is consistent with evidences indicating that glucocorticoids may cause a selective suppression of the Th1 immune response (e.g. interferon gamma), and a Th2 shift, rather than generalized immunosuppression⁴⁵. At T4 the scenery appeared to be more complex: overall, less cytokines were regulated respect to T3, probably due to the 6 days suspension of the treatment, and some of them showed a double effect acting as pro- or anti-inflammatory depending on the context (e.g. IL6, whose receptor was up-regulated⁴⁶). However, most of them seemed to be important for T and NK cell survival, development and homeostasis⁴⁷⁻⁴⁸. Interestingly, microarray analyses evidenced IL7 receptor alpha as a glucocorticoid-inducible gene associated with enhanced IL-7 mediated signaling and function⁴⁹. Toll-like receptor (TLR) pathway (11 genes) and MAPKK pathway (22 genes) were regulated at T4 as well, thereby confirming a PDN effect on innate components of immunity¹². Indeed, glucocorticoids were shown to regulate the expression of TLRs (e.g. TLR2, TLR3 and TLR4) in immune cells thereby affecting inflammation and host defense mechanisms⁵⁰. Many genes implicated in transcription regulation are also altered by PDN treatment at both sampling times, most of which are involved in the control of PBMCs proliferation and/or differentiation (e.g., bone

morphogenic protein 4, peroxisome proliferator-activated receptor-gamma, hypoxia-inducible factor 1-alpha, activin A receptor type 1). For instance, the up-regulation of peroxisome proliferator-activated receptor-gamma observed at T3, may support for the inhibition of cytokines that are important for Th1-cell differentiation⁵¹. Apart from confirming the effects on PDN on the maintenance of immunologic homeostasis, differentiation of T-lymphocytes population and its effect on both innate and adaptive arms of immune system¹¹, what emerged from our investigation is that despite a mild effect obtained by PDN treatment on bovine thymus, PBMCs showed a more pronounced responsiveness against the treatment. This clear corticosteroid signature could allow to propose this matrix as an useful tool to identify animals potentially treated with PDN. In particular, the application of bioinformatics tools as PAM allowed to correctly discriminate 93% of samples using only 36 predictive genes that could be proposed as potential biomarkers not only during the illicit treatment with PDN but also after 6 days suspension.

PDN and its metabolites are no longer detectable by LC-MS/MS methods in biological fluids. Moreover, they do not induce any histological alterations in thymus, differently from DEX treatments¹¹. The present study confirmed the usefulness of an integrated approach to the investigation of PDN abuse in beef cattle, as previously reported^{12,52}. Concerning indirect biomarkers, blood chemistry analysis and histological techniques have been proposed and adopted as alternative screening methods for the prevention of CSs abuse. Recent studies revealed the feasibility of transcriptome analysis using DNA-microarrays as a screening tool to identify the biological response to different illegal drugs, and could be useful to flank the official methods in detecting the use of anabolic compounds in beef cattle^{12,52-55}.

Histological investigations on epididymal tissues could represent a promising marker for PDN treatment in beef cattle. This simple and cheap analysis, in association with transcriptomic approach and TEM observation, could be used as a screening method in order to identify animals worthy of further investigation with official methods. Moreover, PBMCs markers suggested in this work could be very useful to monitor the illicit treatment in livestock.

Conflict of interest statement

None of the authors has any financial or personal relationships that could inappropriately influence or bias the content of the paper.

Acknowledgments

The authors gratefully acknowledge the Centro di Referenza di Patologia Comparata “Bruno Maria Zaini” (Torino, Italy).

Funding sources

This work was partially funded by the Ministero delle Politiche Agricole e Forestali, project “SAFORISK - Prevenzione dell’uso di anabolizzanti in zootecnia. Creazione di un Marchio a difesa degli allevamenti italiani” (D.M. 2089/09, 29th of January 2009).

References

1. Kandeel, M.; Balaha, M.; Inagaki, N.; Kitade, Y. Current and future asthma therapies. *Drugs Today (Barc)*. **2013**, *49*, 325-339.
2. Gottardo, F.; Brscic, M.; Pozza, G.; Ossensi, C.; Contiero, B.; Marin, A.; Cozzi, G. Administration of dexamethasone per os in finishing bulls. I. Effects on productive traits, meat quality and cattle behavior as indicator of welfare. *Animal* **2008**, *2*, 1073-1079.
3. EEC Commission Regulation N° 37/2010. Official Journal of the European Community L 15:1.
4. PNR, 2010. Relazione finale Piano Nazionale per la ricerca di Residui 2010. http://www.salute.gov.it/imgs/C_17_pubblicazioni_1637_allegato.pdf
5. PNR, 2009. Relazione finale Piano Nazionale Residui 2009. http://www.salute.gov.it/imgs/c_17_pubblicazioni_1296_allegato.pdf
6. Biolatti, B.; Bollo, E.; Cannizzo, F.T.; Zancanaro, G.; Tarantola, M.; Dacasto, M.; Cantiello, M.; Carletti, M.; Biolatti, P.G.; Barbarino, G. Effects of low-dose dexamethasone on thymus morphology and immunological parameters in veal calves. *J. Vet. Med. A Physiol. Pathol. Clin. Med.* **2005**, *52*, 202-208.
7. Cannizzo, F.T.; Miniscalco, B.; Riondato, F.; Bollo, E.; Barbarino, G.; Giorgi, P.; Mazzini, C.; Biolatti, B. Effects of anabolic and therapeutic doses of dexamethasone on thymus morphology and apoptosis in veal calves. *Vet. Rec.* **2008**, *163*, 448-452.
8. Vascellari, M.; Pozza, G.; Poppi, L.; Capello, K.; Angeletti, R.; Ravarotto, L.; Andrighetto, I.; Mutinelli, F. Evaluation of indirect biomarkers of corticosteroids use as illegal growth promoters in beef cattle. *Vet. Rec.* **2008**, *163*, 147-152.
9. Cannizzo, F.T.; Spada, F.; Benevelli, R.; Nebbia, C.; Giorgi, P.; Brina, N.; Bollo, E.; Biolatti, B. Thymus atrophy and regeneration following dexamethasone administration to beef cattle. *Vet. Rec.* **2010**, *167*, 338-343.
10. Vascellari, M.; Capello, K.; Stefani, A.; Biancotto, G.; Moro, L.; Stella, R.; Pozza, G.; Mutinelli, F. Evaluation of thymus morphology and serum cortisol concentration as indirect biomarkers to detect low-dose dexamethasone illegal treatment in beef cattle. *BMC Vet. Res.* **2012**, *8*, 129.
11. Cannizzo, F.T.; Capra, P.; Divari, S.; Ciccotelli, V.; Biolatti, B.; Vincenti, M. Effects of low-dose dexamethasone and prednisolone long term administration in beef calf: chemical and morphological investigation. *Anal. Chim. Acta* **2011**, *700*, 95-104.
12. Cannizzo, F.T.; Pegolo, S.; Starvaggi Cucuzza, L.; Bargelloni, L.; Divari, S.; Franch, R.; Castagnaro, M.; Biolatti, B. Gene expression profiling of thymus in beef cattle treated with prednisolone. *Res. Vet. Sci.* **2013**, *95*, 540-547.
13. EEC - Directive 2003/74/EC of the European Parliament and of the Council of 22 September 2003 amending Council Directive 96/22/EC concerning the prohibition on the use in stockfarming of certain substances having a hormonal or thyrostatic action and of beta-agonists. [http://eur-lex.europa.eu/legal-content/EN/ALL/?uri=CELEX:32003L0074\(01/03/16\)](http://eur-lex.europa.eu/legal-content/EN/ALL/?uri=CELEX:32003L0074(01/03/16))
14. Moiré, N.; Roy, O.; Gardey, L. Effects of dexamethasone on distribution and function of peripheral mononuclear blood cells in pneumonic calves. *Vet. Immunol. Immunopathol.* **2002**, *87*, 459-466.
15. Kubista, M.; Andrade, J. M.; Bengtsson, M.; Forootan, A.; Jonák, J.; Lind, K.; Sindelka, R.; Sjöback, R.; Sjögreen, B.; Strömbom, L.; Ståhlberg, A.; Zoric, N. The real-time polymerase chain reaction. *Mol. Aspects Med.* **2006**, *27*, 95-125.
16. Rozen, S.; Skaletsky, H. J. Primer3 on the WWW for general users and for biologist programmers. In: *Bioinformatics methods and protocols: Methods in molecular biology*; Krawetz S., Misener S., Eds.; Humana Press: Totowa, NJ, 2000; pp. 365-386.

17. Divari, S.; Pregel, P.; Cannizzo, F.T.; Starvaggi Cucuzza, L.; Brina, N.; Biolatti, B. Oxytocin precursor gene expression in bovine skeletal muscle is regulated by 17 β -oestradiol and dexamethasone. *Food Chem.* **2013**, *141*, 4358-4366.
18. Bustin, S. A.; Benes, V.; Garson, J. A.; Hellemans, J.; Hugget, J.; Kubista, M.; Mueller, R.; Nolan, T.; Pfaffl, M.W.; Shipley, G.L.; Vandesompele, J.; Wittwer, C.T. The MIQE guidelines: Minimum information for publication of quantitative real-time PCR experiments. *Clin. Chem.* **2009**, *55*, 611-622.
19. Livak, K. J.; Schmittgen, T.D. Analysis of relative gene expression data using real-time quantitative PCR and the 2(-Delta Delta C(T)) method. *Methods* **2001**, *25*, 402-408.
20. Pfaffl, M. W. Quantification strategies in real-time PCR. In: *A-Z of quantitative PCR*; Bustin, S. A., Ed.; International University Line (IUL): La Jolla, CA, USA, 2004, pp. 87-112.
21. Wong, M. L.; Medrano, J. F. Real-time PCR for mRNA quantitation. *Biotechniques* **2005**, *39*, 75-85.
22. Edgar, R.; Domrachev, M.; Lash, A.E. Gene Expression Omnibus: NCBI gene expression and hybridization array data repository. *Nucleic Acids Res.* **2002**, *30*, 207-210.
23. Saeed, A.I.; Bhagabati, N.K.; Braisted, J.C.; Liang, W.; Sharov, V.; Howe, E.A.; Li, J.; Thiagarajan, M.; White, J.A.; Quackenbush, J. TM4 microarray software suite. *Methods Enzymol.* **2006**, *411*, 134-193.
24. Tibshirani, R.; Hastie, T.; Narasimhan, B.; Chu, G. Diagnosis of multiple cancer types by shrunk centroids of gene expression. *Proc. Natl. Acad. Sci. USA* **2002**, *99*, 6567-6572.
25. Caballero, J.; Frenette, G.; Sullivan, R. Post testicular sperm maturational changes in the bull: important role of the epididymosomes and prostasomes. *Vet. Med. Int.* **2010**, *2011*, 757194.
26. Schwarz, A.; Wennemuth, G.; Post, H.; Brandenburger, T.; Aumüller, G.; Wilhelm, B. Vesicular transfer of membrane component to bovine epididymal spermatozoa. *Cell Tissue Res.* **2013**, *353*, 549-561.
27. Starvaggi Cucuzza, L.; Biolatti, B.; Sereno, A.; Cannizzo, F.T. Regucalcin Expression as a Diagnostic Tool for the Illicit Use of Steroids in Veal Calves. *J. Agric. Food Chem.* **2015**, *63*, 5702-5706.
28. Ludwig, S.K.; Smits, N.G.; Cannizzo, F.T.; Nielen, M.W. Potential of treatment-specific protein biomarker profiles for detection of hormone abuse in cattle. *J. Agric. Food Chem.* **2013**, *61*, 4514-4519.
29. Divari, S.; Cannizzo, F.T.; Uslenghi, F.; Pregel, P.; Mulasso, C.; Spada, F.; De Maria, R.; Biolatti, B. Corticosteroid hormone receptors and prereceptors as new biomarkers of the illegal use of glucocorticoids in meat production. *J. Agric. Food Chem.* **2011**, *59*, 2120-2125.
30. Regal, P.; Blokland, M.H.; Fente, C.A.; Sterk, S.S.; Cepeda, A.; van Ginkel, L.A. Evaluation of the discriminative potential of a novel biomarker for estradiol treatments in bovine animals. *J. Agric. Food Chem.* **2015**, *63*, 370-378.
31. Giantin, M.; Lopparelli, R.M.; Zancanella, V.; Martin, P.G.; Polizzi, A.; Gallina, G.; Gottardo, F.; Montesissa, C.; Ravarotto, L.; Pineau, T.; Dacasto, M. Effects of illicit dexamethasone upon hepatic drug metabolizing enzymes and related transcription factors mRNAs and their potential use as biomarkers in cattle. *J. Agric. Food Chem.* **2010**, *58*, 1342-1349.
32. Denison, F.C.; Smith, L.B.; Muckett, P.J.; O'Hara, L.; Carling, D.; Woods, A. LKB1 is an essential regulator of spermatozoa release during spermiation in the mammalian testis. *PLoS One* **2011**, *6*, e28306.
33. Song, J.; Sapi, E.; Brown, W.; Nilsen, J.; Tartaro, K.; Kacinski, B.M.; Craft, J.; Naftolin, F.; Mor, G. Roles of Fas and Fas ligand during mammary gland remodeling. *J. Clin. Invest.* **2000**, *106*, 1209-1220.

34. Nagata, S. Fas and Fas ligand: a death factor and its receptor. *Adv. Immunol.* **1994**, *57*, 129-144.
35. Flegel, C.; Manteniotis, S.; Osthold, S.; Hatt, H.; Gisselmann, G. Expression profile of ectopic olfactory receptors determined by deep sequencing. *PLoS One* **2013**, *8*, e55368.
36. Spehr, M.; Schwane, K.; Riffell, J.A.; Zimmer, R.K.; Hatt, H. Odorant receptors and olfactory-like signaling mechanisms in mammalian sperm. *Mol. Cell. Endocrinol.* **2006**, *250*, 128-136.
37. Parthasarathy, C.; Yuvaraj, S.; Ilangovan, R.; Janani, P.; Kanagaraj, P.; Balaganesh, M.; Natarajan, B.; Sittadjody, S.; Balasubramanian, K. Differential response of Leydig cells in expressing 11 β -HSD type I and cytochrome P450 aromatase in male rats subjected to corticosterone deficiency. *Mol. Cell. Endocrinol.* **2009**, *311*, 18-23.
38. Leung, G.S.; Kawai, M.; Tai, J.K.; Chen, J.; Bandiera, S.M.; Chang, T.K. Developmental expression and endocrine regulation of CYP1B1 in rat testis. *Drug Metab. Dispos.* **2009**, *37*, 523-528.
39. Lopparelli, R.M.; Zancanella, V.; Giantin, M.; Ravarotto, L.; Cozzi, G.; Montesissa, C.; Dacasto, M. Constitutive expression of drug metabolizing enzymes and related transcription factors in cattle testis and their modulation by illicit steroids. *Xenobiotica* **2010**, *40*, 670-680.
40. Lopparelli, R.M.; Zancanella, V.; Giantin, M.; Ravarotto, L.; Pozza, G.; Montesissa, C.; Dacasto, M. Steroidogenic enzyme gene expression profiles in the testis of cattle treated with illicit growth promoters. *Steroids* **2011**, *76*, 508-516.
41. Pegolo, S.; Cannizzo, F.T.; Biolatti, B.; Castagnaro, M.; Bargelloni, L. Transcriptomic profiling as a screening tool to detect trenbolone treatment in beef cattle. *Res. Vet. Sci.* **2014**, *96*, 472-481.
42. Pegolo, S.; Di Camillo, B.; Montesissa, C.; Cannizzo, F.T.; Biolatti, B.; Bargelloni, L. Toxicogenomic markers for corticosteroid treatment in beef cattle: integrated analysis of transcriptomic data. *Food Chem. Toxicol.* **2015**, *77*, 1-11.
43. Antov, A.; Yang, L.; Vig, M.; Baltimore, D.; Van Parijs, L. Essential role for STAT5 signaling in CD25⁺CD4⁺ regulatory T cell homeostasis and the maintenance of self-tolerance. *J. Immunol.* **2003**, *171*, 3435-3441.
44. Kolbus, A.; Blázquez-Domingo, M.; Carotta, S.; Bakker, W.; Luedemann, S.; von Lindern, M.; Steinlein, P.; Beug, H. Cooperative signaling between cytokine receptors and the glucocorticoid receptor in the expansion of erythroid progenitors: molecular analysis by expression profiling. *Blood* **2003**, *102*, 3136-3146.
45. Elenkov, IJ. Glucocorticoids and the Th1/Th2 balance. *Ann. NY Acad. Sci.* **2004**, *1024*, 138-146.
46. Scheller, J.; Chalaris, A.; Schmidt-Arras, D.; Rose-John, S. The pro- and anti-inflammatory properties of the cytokine interleukin-6. *Biochim. Biophys. Acta* **2011**, *1813*, 878-888.
47. Rathmell, J.C.; Farkash, E.A.; Gao, W.; Thompson, C.B. IL-7 enhances the survival and maintains the size of naive T cells. *J. Immunol.* **2001**, *167*, 6869-6876.
48. Ranson, T.; Vosshenrich, C.A.; Corcuff, E.; Richard, O.; Müller, W.; Di Santo, J.P. IL-15 is an essential mediator of peripheral NK-cell homeostasis. *Blood* **2003**, *101*, 4887-4893.
49. Franchimont, D.; Galon, J.; Vacchio, M.S.; Fan, S.; Visconti, R.; Frucht, D.M.; Geenen, V.; Chrousos, G.P.; Ashwell, J.D.; O'Shea, J.J. Positive effects of glucocorticoids on T cell function by up-regulation of IL-7 receptor α . *J. Immunol.* **2002**, *168*, 2212-2218.
50. Galon, J.; Franchimont, D.; Hiroi, N.; Frey, G.; Boettner, A.; Ehrhart-Bornstein, M.; O'Shea, J.J.; Chrousos, G.P.; Bornstein, S.R. Gene profiling reveals unknown enhancing and suppressive actions of glucocorticoids on immune cells. *FASEB J.* **2002**, *16*, 61-71.

51. Daynes, R.A.; Jones, D.C. Emerging roles of PPARs in inflammation and immunity. *Nat. Rev. Immunol.* **2002**, *2*, 748-759.
52. Pegolo, S.; Gallina, G.; Montesissa, C.; Capolongo, F.; Ferraresso, S.; Pellizzari, C.; Poppi, L.; Castagnaro, M.; Bargelloni, L. Transcriptomic markers meet the real world: finding diagnostic signatures of corticosteroid treatment in commercial beef samples. *BMC Vet. Res.* **2012**, *8*, 205.
53. Carraro, L.; Ferraresso, S.; Cardazzo, B.; Romualdi, C.; Montesissa, C.; Gottardo, F.; Patarnello, T.; Castagnaro, M.; Bargelloni, L. Expression profiling of skeletal muscle in young bulls treated with steroidal growth promoters. *Physiol. Genomics* **2009**, *38*, 138-148.
54. Rijk, J.C.; Peijnenburg, A.A.; Hendriksen, P.J.; Van Hende, J.M.; Groot, M.J.; Nielen, M.W. Feasibility of a liver transcriptomics approach to assess bovine treatment with the prohormone dehydroepiandrosterone (DHEA). *BMC Vet. Res.* **2010**, *6*, 44.
55. De Jager, N.; Hudson, N.J.; Reverter, A.; Wang, Y.H.; Nagaraj, S.H.; Cafe, L.M.; Greenwood, P.L.; Barnard, R.T.; Kongsuwan, K.P.; Dalrymple, B.P. Chronic exposure to anabolic steroids induces the muscle expression of oxytocin and a more than fiftyfold increase in circulating oxytocin in cattle. *Physiol. Genomics* **2011**, *43*, 467-478.

Figure legends

Fig. 1. Protocol of PDN treatment and PBMCs collection times. Beef calves were assigned to two experimental groups: Group P was administered prednisolone acetate (PA, Novosterol, Ceva Vetem spa, Italy) 30 mg day⁻¹ *per os* for 35 days; Group K represented the control group. Six days after drug withdrawal the animals were slaughtered.

Fig. 2. Semithin sections of testis and epididymis stained with toluidine blue (a, c, e: controls; b, d, f: treated). a, b testis samples; c-f epididymis samples.

a, c, e: Control animal: normal testis and epididymis with luminal spermatozoa scattered amongst the aposomes.

b, d, f: PDN treated animal: prominent vacuolization of the seminiferous epithelium near the basement membrane. In epididymis spermatozoa concentration decreased significantly up to disappear, and this reduction was accompanied by an increased presence of cellular debris (bar 10 µm). Bm=Basement membrane.

Fig. 3 Transmission electron micrographs of:

a-d: Treated animal germinal epithelium: cytoplasmic shrinkage, extensive round spermatid exfoliation and atypical residual bodies in the luminal surface (rb). Degenerative changes in round and elongated spermatids (arrows) (–a: bar 10µm; b, c: bar 5 µm).

e-f: Epithelium of epididymis in control animals: aposomes (AP) found in the epididymal lumen anchoring the sperm nucleus (e: bar 5 µm). Epididymosomes represented by a heterogeneous variety of vesicles (asterisk) (f: bar 1 µm).

g-h: Treated animal epididymis: columnar epithelial cells showing microvilli (mv) and apical blebs (ab) (g: bar 5 µm). Ultrastructure of an aposome (AP) anchored to an immature sperm cell with swelling of sperm head plasma membrane (asterisk) (h: bar 5 µm). Basement membrane (Bm),

spermatogonia (Sg), Sertoli cell (Sc), spermatocytes (Sp), elongated spermatides (eS), round spermatides (rS) and residual bodies (rb).

Fig. 4. Graphic representation of the distribution of the mean number of Sertoli cells, immature spermatozoa, round and elongated spermatids, spermatocytes, and spermatogonia per tubule section (P = prednisolone; K = control; * $p < 0.05$)

Fig. 5. Plot of cross-validated probabilities for sample classification using DEG (t-test). On x-axis individual samples: 1–14 negative controls (K), 15–30 PDN-treated animals (P); on y-axis the probability of being classified as controls (diamonds) or treated (squares); training error 0.03.

Table 1

DEG obtained from t-test analysis of testis, skeletal muscle and PBMCs samples

	Skeletal muscle	Testis	PBMCs (T3)	PBMCs (T4)
Up-regulated	64	84	539	768
Down-regulated	69	49	368	648

p<0.05, FC≥1.5

Table 2

DEG obtained from t-test analysis of testis samples from bovine treated with PDN.

Identifier	Gene	FC
<i>Olfactory transduction</i>		
XM_593044	Olfactory receptor 6B2 (<i>LOC515090</i>)	-1.6
XM_591408	Olfactory receptor, family 52, subfamily M, member 1 (<i>OR52M1</i>)	1.9
XM_864501	Olfactory receptor, family 6, subfamily C, member 75 (<i>OR6C75</i>)	1.8
XM_582572	Olfactory receptor, family 2, subfamily AG, member 1 (<i>OR2AG1</i>)	1.6
AF074014	Cyclic nucleotide-gated cation channel beta-1 isoform c (<i>CNGB1</i>)	1.6
XM_003584236	Olfactory receptor 8G1-like (<i>LOC616755</i>)	1.5
<i>Calcium homeostasis</i>		
NM_001192710	Cholinergic receptor, nicotinic, alpha 2 (neuronal) (<i>CHRNA2</i>)	2.3
NM_173954	Parathyroid hormone (<i>PTH</i>)	1.8
U81159	Magnesium-dependent calcium inhibitable phosphatase (<i>MCPP</i>)	1.8
XM_608438	Calcium channel, voltage-dependent, alpha 2/delta subunit 4 (<i>CACNA2D4</i>)	1.7
NM_173957	Regucalcin (senescence marker protein-30) (<i>RGN</i>)	-1.6
XM_614307	5-Hydroxytryptamine (serotonin) receptor 3B, ionotropic (<i>HTR3B</i>)	1.5
<i>Xenobiotics metabolism</i>		
NM_173993	Aryl hydrocarbon receptor nuclear translocator (<i>ARNT</i>)	-1.5
NM_174638	Cytochrome P450, subfamily XI B, polypeptide 1 (<i>CYP11B2</i>)	2.8
XM_864665	Sulfotransferase family, cytosolic, 1C, member 2 (<i>SULT1C2</i>)	1.7
NM_001075322	Cytochrome P450, family 4, subfamily F, polypeptide 2 (<i>CYP4F2</i>)	1.5
XM_591370	Cytochrome P450, family 24, subfamily A, polypeptide 1-like, transcript variant 2 (<i>CYP24A1</i>)	1.5
<i>Immune system regulation</i>		
XR_083623	Recombination activating gene 1 activating protein 1-like (<i>LOC520463</i>) miscRNA	-4.1
NM_001205850	Cytoplasmic FMR1 interacting protein 2 (<i>CYFIP2</i>)	-3.1
NM_001101251	Interferon, gamma-inducible protein 30 (<i>IFI30</i>)	-1.5

NM_001075142	Interleukin 4 receptor (<i>IL4R</i>)	-1.5
XM_003587343	Leukocyte immunoglobulin-like receptor subfamily A member 6-like (<i>LOC790255</i>)	1.9
XR_082749	Colony stimulating factor 3 receptor (<i>CSF3R</i>)	1.7
NM_001105388	IL2-inducible T-cell kinase (<i>ITK</i>)	1.6
XM_584848	Immunoglobulin superfamily, member 21-like (<i>IGSF21</i>)	1.5
NM_001045933	Forkhead box P3 (<i>FOXP3</i>)	1.5
NM_001075291	Zinc finger CCCH-type containing 8 (<i>ZC3H8</i>)	1.5
NM_001075807	CKLF-like MARVEL transmembrane domain containing 2 (<i>CMTM2</i>)	1.5
XM_002699526	Interferon regulatory factor 2 binding protein 1	1.5
<hr/> <i>Apoptosis and cell cycle regulation</i> <hr/>		
NM_001205850	Cytoplasmic FMR1 interacting protein 2 (<i>CYFIP2</i>)	-3.1
NM_173957	Regucalcin (senescence marker protein-30) (<i>RGN</i>)	-1.6
BC149759	Tumor necrosis factor receptor superfamily member 10A (<i>TNFRSF10A</i>)	2.0
NM_001192518	Unc-5 homolog D (<i>C. elegans</i>) (<i>UNC5D</i>)	1.9
NM_001098859	Fas ligand (TNF superfamily, member 6) (<i>FASLG</i>)	1.5
BM255900	Cyclin-dependent kinase 6 (<i>CDK6</i>)	1.5
CB427007	Cyclin-T1 (<i>CCNT1</i>)	1.5
NM_001046178	Protein phosphatase 1, regulatory subunit 15A (<i>PPP1R15A</i>)	1.5
<hr/> p<0.05, FC≥1.5 <hr/>		

Table 3

DEG obtained from t-test analysis of skeletal muscle samples from bovine treated with PDN.

Identifier	Gene	FC
<i>Xenobiotic metabolism</i>		
NM_001075823	Sulfotransferase family cytosolic 1B member 1 (<i>SULT1B1</i>)	-2.1
NM_174530	Cytochrome P450, family 2, subfamily E, polypeptide 1 (<i>CYP2E1</i>)	1.7
<i>Cell cycle regulation</i>		
NM_001076062	Cell cycle associated protein 1 (<i>CAPRIN1</i>)	-1.5
NM_001083449	Cell death-inducing DFFA-like effector a (<i>CIDEA</i>)	1.9
NM_173954	Zygote arrest 1-like (<i>ZAR1L</i>)	1.8
NM_001206050	Meteorin, glial cell differentiation regulator-like (<i>METRNL</i>)	1.7
NM_001101183	Transforming growth factor, beta 3 (<i>TGFB3</i>)	1.5
<i>Cytokine activity</i>		
NM_174356	Interleukin 12B (<i>IL12B</i>)	-1.5
NM_174006	Chemokine (C-C motif) ligand 2 (<i>CCL2</i>)	3.9
NM_174007	Chemokine (C-C motif) ligand 8 (<i>CCL8</i>)	2.2
p<0.05, FC≥1.5		

Table 4.

Biological processes, molecular functions and KEGG pathways significantly enriched in T3 PBMCs from PDN group animals using the list of DEG (t-test).

Category	Count	PValue	FE	FDR
GO_BP positive regulation of transcription, DNA-dependent	19	3E-04	3E+00	0.58
GO_BP positive regulation of RNA metabolic process	19	3E-04	3E+00	0.58
GO_BP positive regulation of transcription	21	5E-04	2E+00	0.81
GO_BP positive regulation of macromolecule metabolic process	26	8E-04	2E+00	1.38
GO_BP positive regulation of gene expression	21	8E-04	2E+00	1.39
GO_BP regulation of transcription from RNA polymerase II promoter	22	1E-03	2E+00	1.77
GO_BP positive regulation of transcription from RNA polymerase II promoter	16	1E-03	3E+00	1.84
GO_BP positive regulation of nucleobase, nucleoside, nucleotide and nucleic acid metabolic process	21	1E-03	2E+00	2.46
GO_BP positive regulation of macromolecule biosynthetic process	22	2E-03	2E+00	2.88
GO_BP regulation of transcription, DNA-dependent	43	2E-03	2E+00	3.28
GO_BP positive regulation of nitrogen compound metabolic process	21	2E-03	2E+00	3.50
GO_BP positive regulation of cellular biosynthetic	22	3E-03	2E+00	4.41

	process				
GO_BP	regulation of RNA metabolic process	43	3E-03	2E+00	5.01
GO_BP	positive regulation of biosynthetic process	22	3E-03	2E+00	5.15
GO_BP	heart development	11	6E-03	3E+00	9.32
GO_BP	negative regulation of cell proliferation	12	7E-03	3E+00	11.59
GO_BP	regulation of transcription	53	1E-02	1E+00	16.02
GO_BP	positive regulation of cell differentiation	10	1E-02	3E+00	17.51
GO_BP	regulation of cell proliferation	20	2E-02	2E+00	25.21
GO_BP	regulation of growth	12	2E-02	2E+00	26.01
GO_BP	BMP signaling pathway	4	2E-02	7E+00	26.04
GO_BP	positive regulation of developmental	11	2E-02	2E+00	27.98
	process				
GO_BP	transmembrane receptor protein	6	2E-02	4E+00	28.66
	serine/threonine kinase signaling pathway				
GO_BP	placenta development	5	3E-02	4E+00	36.29
GO_BP	tRNA modification	4	3E-02	6E+00	37.31
GO_BP	fat cell differentiation	5	3E-02	4E+00	40.42
GO_BP	pattern specification process	9	4E-02	2E+00	46.01
GO_BP	tRNA processing	6	5E-02	3E+00	54.72
GO_MF	cytokine binding	12	4E-05	5E+00	0.06
GO_MF	sequence-specific DNA binding	24	3E-04	2E+00	0.50
GO_MF	transcription factor activity	29	6E-04	2E+00	0.89
GO_MF	transcription regulator activity	41	8E-04	2E+00	1.09
GO_MF	cytokine receptor activity	6	7E-03	5E+00	9.36
GO_MF	C-C chemokine binding	5	7E-03	6E+00	10.03

GO_MF	C-C chemokine receptor activity	5	7E-03	6E+00	10.03
GO_MF	chemokine receptor activity	5	1E-02	5E+00	17.53
GO_MF	chemokine binding	5	2E-02	5E+00	23.73
GO_MF	protein dimerization activity	15	3E-02	2E+00	38.01
GO_MF	DNA binding	45	4E-02	1E+00	44.04
KEGG	Cytokine-cytokine receptor interaction	18	2E-04	3E+00	0.24
KEGG	Systemic lupus erythematosus	11	4E-04	4E+00	0.52
KEGG	Chemokine signaling pathway	12	4E-02	2E+00	39.63

GO: Gene Ontology; BP: Biological Processes; MF: Molecular Functions; KEGG: KEGG

pathways; FE: Fold Enrichment; FDR: False Discovery Rate

Table 5.

Biological processes, molecular functions and KEGG pathways significantly enriched in T4 PBMCs from PDN group animals using the list of DEG (t-test).

Category		Count	PValue	FE	FDR
GO_BP	regulation of transcription, DNA-dependent	56	0.004	1.439	7.2
GO_BP	regulation of phosphorylation	20	0.004	2.009	7.3
GO_BP	regulation of transcription	74	0.006	1.339	9.3
GO_BP	regulation of phosphorus metabolic process	20	0.006	1.940	10.5
GO_BP	regulation of phosphate metabolic process	20	0.006	1.940	10.5
GO_BP	regulation of RNA metabolic process	56	0.007	1.406	11.2
GO_BP	regulation of protein kinase activity	14	0.008	2.243	13.4
GO_BP	regulation of transferase activity	15	0.009	2.161	13.5
GO_BP	cell activation	15	0.009	2.161	13.5
GO_BP	positive regulation of transferase activity	11	0.009	2.572	14.3
GO_BP	positive regulation of protein kinase activity	10	0.012	2.641	18.1
GO_BP	regulation of kinase activity	14	0.014	2.102	21.8
GO_BP	cell cycle	25	0.015	1.658	22.2
GO_BP	positive regulation of kinase activity	10	0.016	2.502	24.5
GO_BP	ribonucleoside monophosphate biosynthetic process	5	0.022	4.457	31.4
GO_BP	leukocyte activation	13	0.022	2.060	31.6
GO_BP	regulation of MAP kinase activity	8	0.025	2.716	34.9
GO_BP	transcription	38	0.026	1.415	35.9
GO_BP	ribonucleoside monophosphate metabolic	5	0.033	3.961	43.4

	process				
GO_BP	protein kinase cascade	12	0.036	1.990	46.6
GO_BP	positive regulation of MAP kinase activity	6	0.037	3.169	47.1
GO_BP	MAPKKK cascade	8	0.043	2.427	52.7
GO_BP	ribosome biogenesis	9	0.043	2.252	52.8
GO_MF	phosphoinositide binding	10	3E-04	4E+00	4E-01
GO_MF	phospholipid binding	13	1E-03	3E+00	2E+00
GO_MF	heparin binding	7	1E-02	4E+00	1E+01
GO_MF	N-methyltransferase activity	6	2E-02	4E+00	2E+01
GO_MF	sequence-specific DNA binding	25	2E-02	2E+00	2E+01
GO_MF	transcription regulator activity	47	3E-02	1E+00	3E+01
GO_MF	glycosaminoglycan binding	8	3E-02	3E+00	4E+01
GO_MF	peptide receptor activity	10	3E-02	2E+00	4E+01
GO_MF	peptide receptor activity, G-protein coupled	10	3E-02	2E+00	4E+01
GO_MF	GTPase activity	10	4E-02	2E+00	4E+01
GO_MF	chemokine receptor activity	5	4E-02	4E+00	5E+01
GO_MF	low-density lipoprotein binding	4	5E-02	5E+00	5E+01
KEGG	Intestinal immune network for IgA production	9	0.002	3.637	2.9
KEGG	Cytokine-cytokine receptor interaction	20	0.005	1.966	6.0
KEGG	Toll-like receptor signaling pathway	11	0.028	2.163	28.5
KEGG	MAPK signaling pathway	22	0.030	1.600	30.6

GO: Gene Ontology; BP: Biological Processes; MF: Molecular Functions; KEGG: KEGG

pathways; FE: Fold Enrichment; FDR: False Discovery Rate

Table 6

Most predictive genes identified by PAM software.

ProbeID	GenBank Accession	GeneSymbol	Description
A_73_100298	NM_001102271	<i>CLK1</i>	Bos taurus CDC-like kinase 1 (CLK1)
A_73_100941	XM_015475453	<i>FBRSL1</i>	Bos taurus fibrosin-like1
A_73_100990	NM_001037616	<i>HMGB2</i>	Bos taurus high mobility group box 2
A_73_101271	NM_001114192	<i>HSPA4</i>	Bos taurus heat shock 70kDa protein 4
A_73_101276	NM_001080730	<i>MRPL39</i>	Bos taurus mitochondrial ribosomal protein L39
A_73_103257	NM_001192222	<i>THUMPD2</i>	Bos taurus THUMP domain containing 2
A_73_103288	BM087726	-	Rep: Pistil extensin like protein - Nicotiana tabacum (Common tobacco), partial (6%)
A_73_103758	NM_001038074	<i>COX4NB</i>	Bos taurus COX4 neighbor
A_73_103832	NM_001045900	<i>PSMD3</i>	Bos taurus proteasome (prosome, macropain) 26S subunit, non-ATPase, 3
A_73_103999	BF041736	-	Rep: 3-oxoacyl-acyl-carrier protein reductase - Plasmodium yoelii yoelii, partial (5%)
A_73_104896	DV786218	-	HW_Liver_4_D04 Bos taurus CF-24-HW liver cDNA library Bos taurus cDNA
A_73_105049	NM_001035389	<i>ING4</i>	Bos taurus inhibitor of growth family, member 4
A_73_105411	NM_001191328	<i>TSSC1</i>	Bos taurus tumor suppressing subtransferable candidate 1
A_73_106645	NM_001098863	<i>MSMO1</i>	Bos taurus methylsterol monooxygenase 1
A_73_107442	XM_001790523	<i>EXOSC5</i>	Bos taurus exosome component
A_73_108504	NM_001206196	<i>KLHL24</i>	Bos taurus kelch-like 24 (Drosophila)
A_73_110210	XM_001787300	<i>CABLES1</i>	Bos taurus Cdk5 and Abl enzyme substrate 1
A_73_112712	NM_001046136	<i>ABCF2</i>	Bos taurus ATP-binding cassette, sub-family F, member 2
A_73_113837	NM_001101131	<i>MAT2A</i>	Bos taurus methionine adenosyltransferase II, alpha
A_73_114350	XM_002705068	<i>AKNA</i>	Bos taurus AT-hook transcription factor
A_73_115182	NM_001035358	<i>MKNK1</i>	Bos taurus MAP kinase interacting serine/threonine kinase 1
A_73_115262	NM_001038088	<i>NASP</i>	Bos taurus nuclear autoantigenic sperm protein (histone-binding)
A_73_115371	XM_870542	<i>GRK6</i>	Bos taurus similar to G protein-coupled receptor kinase 6
A_73_115718	NM_001191138	<i>ELF2</i>	Bos taurus E74-like factor 2
A_73_116099	NM_178317	<i>TRIB2</i>	Bos taurus tribbles homolog 2 (Drosophila)
A_73_116856	XM_001788896	<i>GPCPD1</i>	Bos taurus glycerophosphocholine phosphodiesterase GDE1 homolog (S. cerevisiae)

A_73_117218	XM_867197	<i>FCHSD2</i>	Bos taurus FCH and double SH3 domains 2, transcript variant X1
A_73_117533	NM_174759	<i>PDCL</i>	Bos taurus phosducin-like
A_73_117749	NM_001083515	<i>TMEM87A</i>	Bos taurus transmembrane protein 87A
A_73_117986	NM_001076257	<i>ARRDC3</i>	Bos taurus arrestin domain containing 3
A_73_119285	NM_001075217	<i>SIRT7</i>	Bos taurus sirtuin 7
A_73_119510	NM_001075558	<i>HERPUD2</i>	Bos taurus HERPUD family member 2
A_73_119516	NM_001206899	<i>MNT</i>	Bos taurus MAX binding protein
A_73_119519	CN442042	-	BE04028A1A06 Normalized and Subtracted bovine embryonic and extraembryonic tissue Bos taurus cDNA clone BE04028A1A06 5
A_73_120487	NM_001045866	<i>BRD2</i>	Bos taurus bromodomain containing 2
A_73_121009	NM_001099065	<i>C16H1orf55</i>	Bos taurus chromosome 16 open reading frame, human C1orf55

Fig. 1

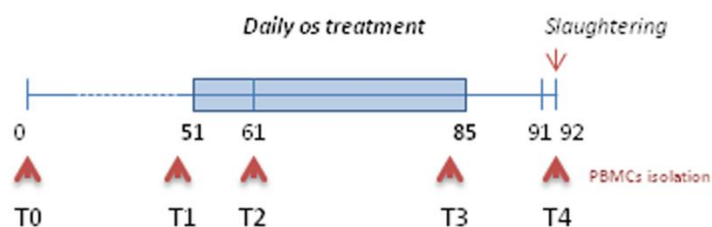


Fig. 2

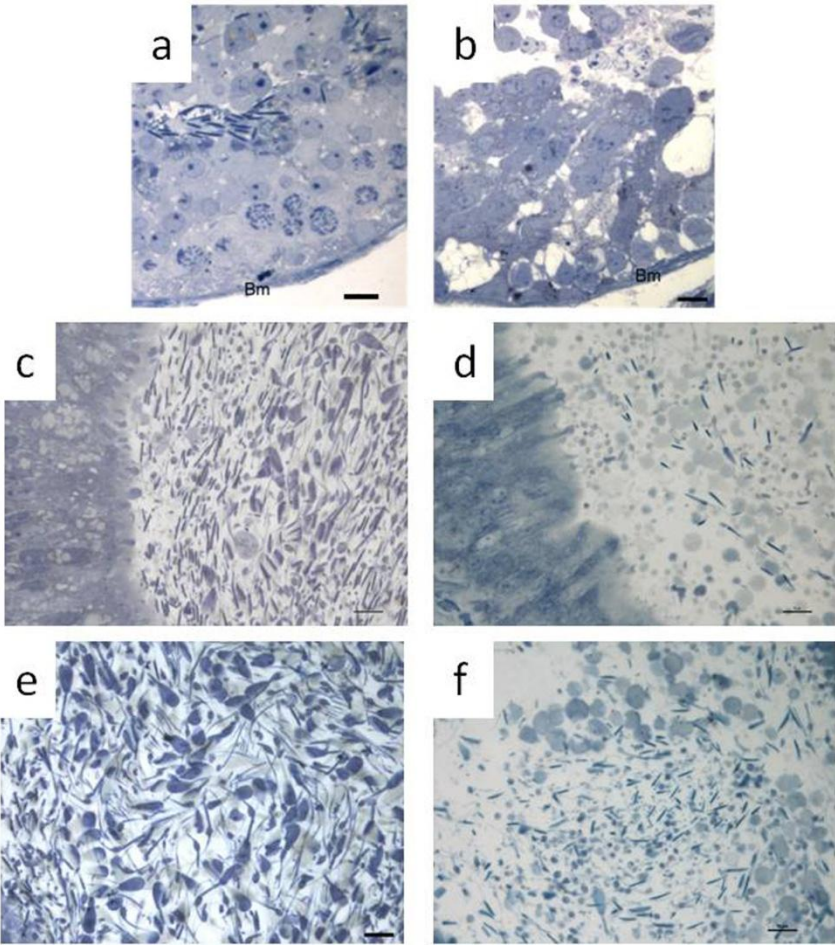


Fig. 3

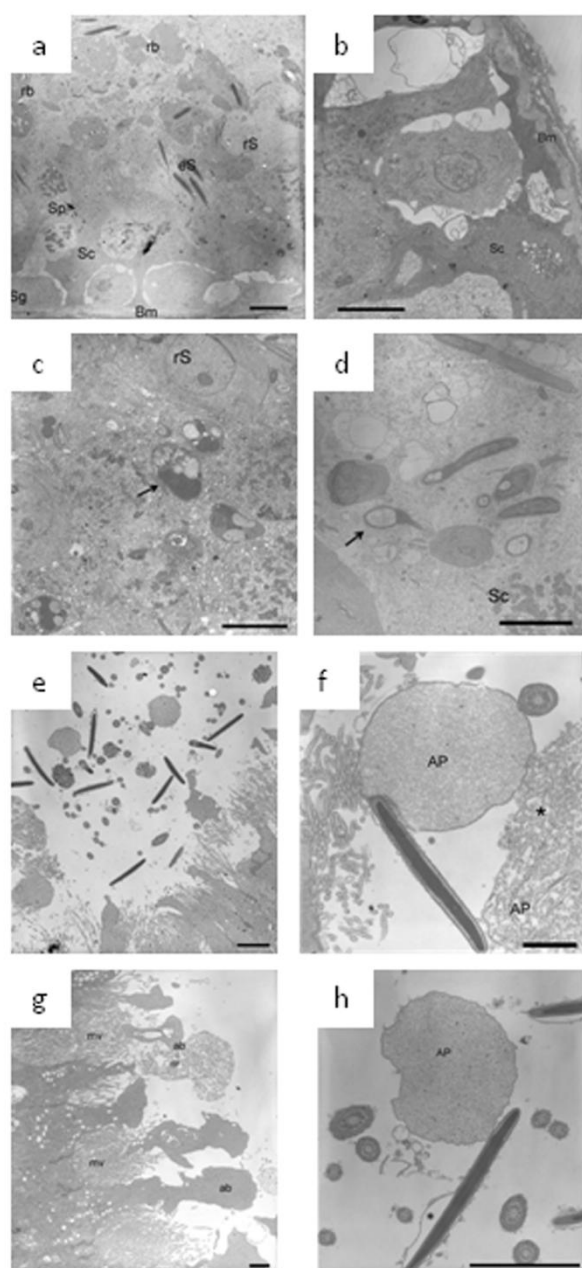


Fig. 4

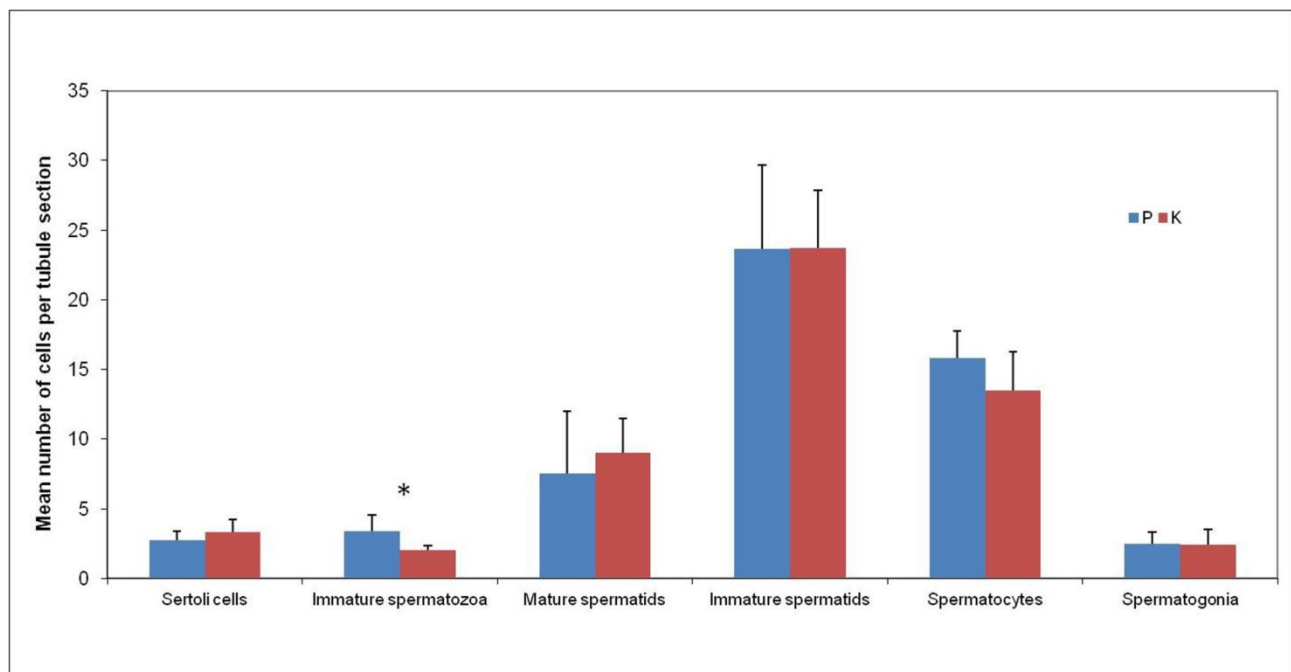
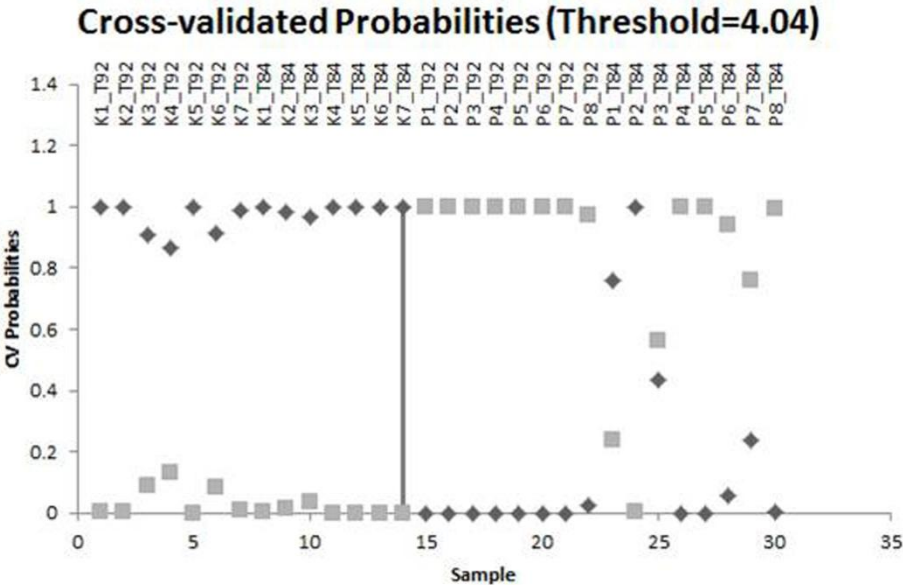


Fig. 5



TOC Graphic

